Dalton Transactions

ROYAL SOCIETY OF CHEMISTRY

PAPER

View Article Online
View Journal | View Issue

Check for updates

Cite this: *Dalton Trans.*, 2024, **53**, 2635

Subphthalocyanines as fluorescence sensors for metal cations†

Mary Angelia Alfred, [a] Kamil Lang, [b] Kaplan Kirakci, [b] Pavel Stuzhin, [c] Petr Zimcik, [a] Jan Labuta *[d] and Veronika Novakova *[a]

Received 16th November 2023,
Accepted 3rd January 2024

DOI: 10.1039/d3dt03839d

rsc.li/dalton

Subphthalocyanines (SubPcs) and their aza-analogues (SubTPyzPzs) are fluorophores with strong orange fluorescence emission; however, their sensing ability towards metal cations remains uncharted. To fill this gap, we have developed an efficient method for introducing aza-crown moieties at the axial position of SubPcs and SubTPyzPzs to investigate the structure–activity relationship for sensing alkali (Li^+, Na^+, K^+) and alkaline earth metal (Ca^{2+}, Mg^{2+}, Ba^{2+}) cations. SubPcs showed better photostability than SubTPyzPzs and even a commonly utilized dye, 6-carboxyfluorescein. Selectivity toward metal cations was driven by the size of the aza-crown, irrespective of the counter anion. The stoichiometry of binding was found to be 1 : 1 in all cases, and the interaction between SubPcs and cations was characterized by the corresponding apparent binding constants (K_a). Notably, an unusually strong interaction of all sensoric SubPcs with Ba^{2+} compared to other studied cations was demonstrated. The role of the surrounding environment, *i.e.* the addition of water or methanol, in sensing cations is shown in detail as well. Selectivity towards K^+ over Na^+ was demonstrated in aqueous media with SubPcs bearing the 1-aza-6-crown-18 moiety in Tween 80 micelles. In this case, a 5-fold increase of the fluorescence quantum yield was observed upon binding K^+ ions. The high brightness, photostability, and sensing activity in aqueous media make SubPc macrocycles promising fluorophores for metal cation sensing.

Introduction

Metal cations are fundamental elements for sustaining plant, animal, and human life. Their absence or increase to toxic levels can cause growth disorders, severe malfunction, or even death.[1,2] Various fluorescent probes are, therefore, being developed to enable their monitoring. Switching such probes on and off is typically driven by photo-induced electron transfer, charge transfer, fluorescence resonance energy transfer, excimer formation or metal-coordination-induced chemical reactions. The details of these switching mechanisms may be found in many reviews.[3–5]

For the recognition of alkali and alkaline earth metal cations, crowns are probably the most suitable hosts, since their selectivity and sensitivity of recognition may be easily tuned by their size, exchange of oxygen for other heteroatoms or attachment of additional binding sites either in the form of a supporting ligand or as a cryptand.[6–10] Wide diversity may be on the other hand found in signalling moieties, since many structurally different fluorophores can be found in the literature.[11,12] Phthalocyanines and especially their aza-analogues have been shown to possess advantageous properties in sensing applications due to their spectral and photophysical properties.[13,14] The lower homologues of phthalocyanines (*i.e.*, subphthalocyanines, SubPcs) and of tetrapyrazinoporphyrazines (SubTPyzPzs), have been used as fluorophores for photochromic switches,[15,16] and as photosensitizers for photodynamic therapy of cancer.[17–21] The great application potential of these macrocycles has been summarized in recent reviews.[22,23] To the best of our knowledge, no aza-crown containing SubPcs and only a limited number of crown containing SubPcs have been successfully prepared with a crown at the peripheral positions[24] or a benzocrown[21] at the axial position. Surprisingly, SubPcs have not yet been studied as fluorescence sensors for cation recognition. Thanks to promising literature

[a]*Faculty of Pharmacy in Hradec Kralove, Charles University, Ak. Heyrovskeho 1203, Hradec Kralove, 500 05 Czech Republic. E-mail: veronika.novakova@faf.cuni.cz*
[b]*Institute of Inorganic Chemistry of the Czech Academy of Sciences, 250 68 Husinec-Řez, Czech Republic*
[c]*Institute of Macroheterocycles, Ivanovo State University of Chemistry and Technology, Sheremetevskij Pr-t 7, 153000 Ivanovo, Russia*
[d]*Research Center for Materials Nanoarchitectonics (MANA), National Institute for Materials Science (NIMS), 1-1 Namiki, Tsukuba, Ibaraki 305-0044, Japan. E-mail: labuta.Jan@nims.go.jp*

†Electronic supplementary information (ESI) available: NMR spectra, effect of the counter anion, stoichiometry studies, summary of obtained apparent binding constants, binding isotherms from fluorescence measurements, effect of water, characterization of micelles, and sensing in water. See DOI: https://doi.org/10.1039/d3dt03839d

notes about these fluorophores in the sensing of pH[25] and fluorides,[26] we decided to investigate the suitability of these macrocycles for cation recognition. We believe that they may extend the range of fluorophores for the visible area (around 590 nm) and that they may be superior to some of the fluorophores that suffer from notable photobleaching (*e.g.*, cyanine dyes). Moreover, the great advantage of these compounds is the possibility of introducing a recognition moiety into the axial position, whereas peripheral sites may be used for tuning the spectral and physicochemical properties.

In this project, we, therefore, aimed to investigate for the first time SubPcs and SubTPyzPzs as signalling moieties for recognition of alkali and alkaline earth metal cations and to prove the sensing principle even in water employing Tween 80 micelles.

Results and discussion

Design and synthesis

The target compounds were designed to possess SubPc or SubTPyzPz as a signalling moiety, which ensures strong fluorescence emission at about 590 and 560 nm, respectively. Phenyl groups attached to the periphery of macrocycles enrich the π-system of the macrocycle, thus shifting the absorption maximum toward red. Both SubPc and SubTPyzPz cores were included to study the effect of aza-substitution. As axial ligands, they carry either 1-aza-4-crown-12, 1-aza-5-crown-15 or 1-aza-6-crown-18 capable of cation recognition. These recognition moieties were attached with a macrocycle through a phenylene linker to minimize the basicity of nitrogen responsible for switching and thus limit undesirable pH sensitivity (see also the discussion below). A control compound (always-ON) with phenol as the axial ligand was also introduced in the study.

Ligands intended to be attached to the axial positions of macrocycles were prepared by a three-step procedure beginning from *p*-bromophenol (Scheme 1, i–iii). Its hydroxy group was protected with a tetrahydropyranyl ether followed by Buchwald–Hartwig coupling with an appropriate aza-crown ether. Finally, the protecting group was removed by acidic hydrolysis. Noteworthily, similar synthetic pathways with methyl as a protecting group and using BBr_3 or HBr for deprotection were successful in our hands as well, but the yields differed significantly at each batch. By the above-mentioned procedure, we obtained the desired ligands **3a–c** repeatedly in overall yields of about 80%.

Precursors **4** and **5** were prepared according to the literature[27–29] but crystallization from benzene and hexane instead of sublimation as a final purification step of **4** was used to get this compound in an improved yield of 78%.

Cyclotrimerization of 4,5-diphenylphthalonitrile (**4**) followed by direct substitution with the respective ligands as a one-pot reaction[25] led to the target macrocycles **6a–d** in yields of about 23% (Scheme 2). Toluene and *p*-xylene were chosen as solvents to avoid chlorination by Cl_2 evolved from BCl_3. The similar conditions applied for 5,6-diphenylpyrazine-2,3-dicarbonitrile (**5**) and ligand **3b** produced the desired SubTPyzPz **7b**, which was, however, found to be less stable than the SubPc analogue **6b**. The decomposition products made the purification difficult, so we obtained **7b** in a yield of only 11%. Based on this experience, we decided to study the (photo)stability of the target derivatives by UV–vis spectroscopy by observing the decrease in the Q band in THF both in the dark or upon light exposure (100 W Xe-ozone free lamp, Newport) (Fig. 1). Sensors **6b** and **7b**, and controls **6d** and **7d** were chosen as model compounds and compared with unsubstituted zinc(II) phthalocyanine (ZnPc) and 6-carboxyfluorescein (FAM) under the same experimental conditions. All the studied derivatives were stable in the dark but decomposed in various degrees under light irradiation. As expected, all the studied derivatives were less stable than ZnPc, which is known

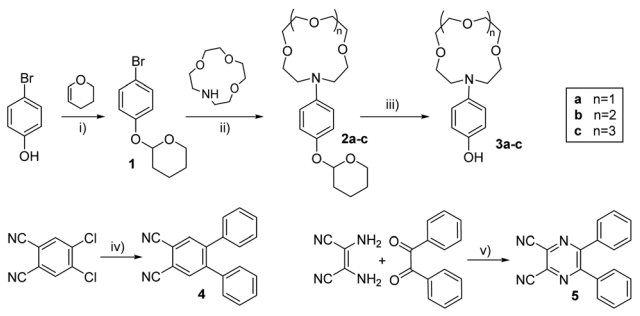

Scheme 1 Synthesis of ligands and precursors – (i) pyridinium 4-toluenesulfonate, anhydrous dichloromethane, argon, room temperature, 2 h, 98%; (ii) $Pd_2(dba)_2$, NaO*t*Bu, Dave Phos, anhydr. toluene, argon, 80 °C, 12 h, 80–92%; (iii) 4-toluenesulfonic acid, methanol, argon atmosphere, room temperature, 2 h, 75–90%; (iv) phenylboronic acid, $PdCl_2(PPh_3)_2$, NaBr, saturated K_2CO_3, dioxane, argon, reflux, 6 h, 78%; (v) acetic acid, reflux, 2 h, 75%.

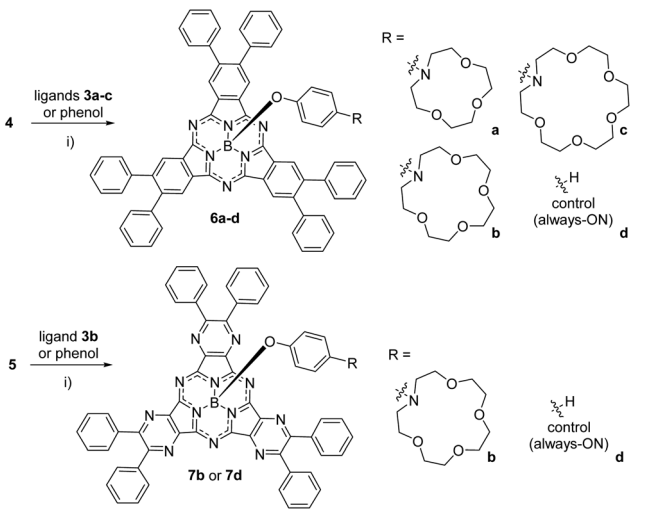

Scheme 2 Synthesis of target macrocycles – (i) BCl_3, *p*-xylene, argon, reflux, 2 h; followed by **3a–c** or phenol, anhydrous toluene, argon, reflux, 12 h, 20–25%.

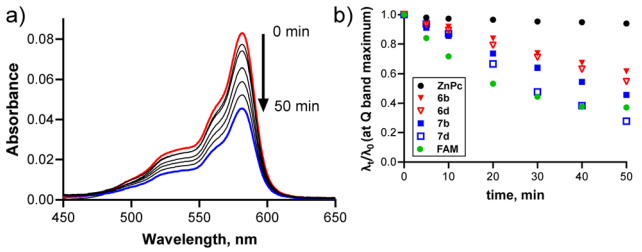

Fig. 1 (a) Changes in the absorption spectra of **6b** (1 μM, THF) upon light irradiation. (b) Normalized decrease of absorption at Q band maximum upon light irradiation (100 W Xe-ozone free lamp, Newport). ZnPc and FAM states for unsubstituted zinc(II) phthalocyanine and 6-carboxyfluorescein, respectively.

for great stability,[30,31] but had better photostability than FAM, which is a common commercially available fluorophore widely used in practice. Obviously, the isosteric replacement of benzenes in SubPcs with pyrazines decreased the stability of the macrocycle. Decomposition produced no distinct spots on the TLC, so the decomposition products could not be determined. From the fact that only a decrease of all absorption bands was observed without the formation of new bands (Fig. S11†), we can only assume that the macrocycle decomposes into low-molecular-weight substances. Many factors influence the photostability of SubPcs and their analogues;[32] thus, a clear explanation is difficult. It is, however, worth noting that long irradiation times were used to clearly observe the differences between compounds. Such light doses are unnecessary in practical applications and were used to test that the target sensor can be considered stable under biologically relevant conditions. Nevertheless, these experiments clearly demonstrated that **6b** is superior to its aza-analogue **7b** in photostability.

UV–vis spectral properties

The characteristic Q band was observed for SubPcs and SubTPyzPzs at about 582 nm and 550 nm, respectively (Table 1). Peripheral phenyls contributed to the π-system of the parent macrocycle, resulting in an ~20 nm red shift in comparison with nonsubstituted macrocycles.[16,25,33] The identical positions of Q bands of **6a–d** indicated no involvement of the axial ligands, which is in accordance with the literature.[25] Since **6b** has a more straightforward purification procedure, better (photo)stability and a red-shifted absorption band (in comparison with **7b**), which is advantageous for any biological experiments, we decided to exclude aza-analogue **7b** from further fluorescence studies and focus on SubPc derivatives only, which seem to have better potential in this application.

Metal cation sensing in tetrahydrofuran

Switching fluorescence between ON and OFF states is typically based on blocking and facilitating a quenching process, respectively. Highly efficient quenching in the OFF state is necessary for good signal-to-noise ratios during analyte detection. In our case, quenching in the OFF state was enabled by photo-induced electron transfer (PET) occurring between a nitrogen in the aza-crown (serving as a donor of electrons) and the SubPc macrocycle (serving as an acceptor). By coordinating the cation to the recognition site of the aza-crown, the lone electron pair of the nitrogen of the aza-crown cannot provide electrons for the PET process, which results in the restoration of strong fluorescence emission. The selectivity of recognition of a given cation should be driven by the size of the aza-crown cavity while the increase in fluorescence (fluorescence enhancement factor, FEF) should be driven by the strength of the coordination of the lone pair to the cation. To prove this mechanism, extensive fluorescence studies were performed.

Upon excitation, SubPcs **6a–c** in THF emitted only weak fluorescence at 593 nm with a Stokes shift of 10 nm.[19,25] Fluorescence quantum yields (Φ_F) were below 0.003 due to highly efficient quenching by PET from the axial nitrogen to the macrocyclic core. The always-ON control **6d** possessed, on the other hand, strong fluorescence emission with the maximum at 592 nm and Φ_F = 0.12 (THF), which correspond to the values published for SubPcs and their analogues (for example Φ_F in acetone for unsubstituted SubPc with the phenoxy group at the axial position, **6d** and **7d** were reported to be 0.18, 0.28 and 0.13, respectively[25]).

Before studying the cation binding to azacrown SubPcs, we focused first on the potential effect of the counter anion. In our previous project with zinc(II) azaphthalocyanines,[9] we described that the sensitivity toward cations is strongly dependent on the counter anion used and increased as follows: $NO_3^- < Br^- < CF_3SO_3^- < ClO_4^- \ll SCN^-$. Extraordinary high sensitivity toward SCN^- resulted from coordination of these anions to the central zinc(II) atom. To select the most suitable counter anion for the current series of SubPcs, we first titrated **6c** as a model compound with different potassium salts (Fig. S12†). Since only negligible differences were observed between thiocyanates and other analytes, we further confirmed the role of zinc(II) in the coordination of the counter anion described in our previous project (because such an interaction is impossible with the central boron atom of **6c**). Overall, the effect of the counter anion was rather limited; therefore, triflate ($CF_3SO_3^-$) was selected as a counter anion for the following experiments due to high Φ_F in the ON state.

The ability of **6a–c** to serve as fluorescence sensors by the above-described mechanism was studied in detail by titrations with Li^+, Na^+, K^+, Mg^{2+}, Ca^{2+} and Ba^{2+} triflates. In the case of sensitive analytes, the stepwise addition of the salt (in a MeOH stock solution) to the THF solution of the studied SubPcs led to a steep increase in fluorescence emission (Table 1, FEF values; Fig. 2c, d and Fig. S16†), reaching a value of Φ_F ~0.1. This Φ_F is close to the value of the always-ON control **6d**, *i.e.* the maximum possible value, which suggests strong binding of particular cations with efficient blocking of PET. Expectedly, no changes were observed in the absorption spectra (Fig. 2a) since electrons of the aza-crown are not involved in the π-conjugated system of the macrocycle.

The stoichiometry of binding of sensitive analytes was studied by both NMR titration studies (Fig. 3, S13 and S14†) and Job's method of continuous variations with fluorescence

Table 1 Spectral and photophysical properties of target derivatives in THF[a]

Compound	Axial ligand	λ_A (nm)	λ_F (nm)	Φ_F (OFF)	Φ_F (ON)	FEF	K_a [b] (M^{-1})
6a	1-Aza-4-crown-12	583	593	0.0023	0.097 Li^+	42	9.9
					0.0023 Na^+	—[c]	—[c]
					0.0023 K^+	—[c]	—[c]
					0.10 Ca^{2+}	43	500
					0.013 Mg^{2+}	5.7	9080
					0.14 Ba^{2+}	61	192 000
6b	1-Aza-5-crown-15	582	593	0.0014	0.0117 Li^+	8.4	5.5
					0.019 Na^+	14	615
					0.0053 K^+	3.8	76
					0.0006 Ca^{2+}	11	58
					0.0041 Mg^{2+}	2.9	520
					0.15 Ba^{2+}	107	13 900
6c	1-Aza-6-crown-18	583	593	0.0022	0.089 Li^+	40	5.7
					0.012 Na^+	5.5	1940
					0.097 K^+	44	36 100 [d]
					0.10 Ca^{2+}	45	11 300
					0.094 Mg^{2+}	43	6 200
					0.090 Ba^{2+}	41	384 000 [e]
6d	Phenol	582	592	0.12	0.11 Li^+	—[c]	—[c]
					0.12 Na^+	—[c]	—[c]
					0.12 K^+	—[c]	—[c]
					0.12 Ca^{2+}	—[c]	—[c]
					0.12 Mg^{2+}	—[c]	—[c]
					0.13 Ba^{2+}	—[c]	—[c]
7b	1-Aza-5-crown-15	550	563				
7d	Phenol	550	562				

[a] Absorption maximum (λ_A), fluorescence emission maximum (λ_F), fluorescence quantum yield (Φ_F) – either without any analyte (Φ_F (OFF)) or at the plateau phase of titration in excess of appropriate salt (in the form of triflates), fluorescence enhancement factor (FEF, *i.e.* the ratio between Φ_F (ON) and Φ_F (OFF)), and apparent association constant (K_a) determined using 1 : 1 host–guest binding model. Φ_F values were determined by a comparison method using rhodamine 6G as the reference (Φ_F = 0.94, EtOH[34]). For the details of titration experiments, see the Experimental part. [b] Values determined from fluorescence emission data. All values have a relative error <15%. [c] No changes in Φ_F of statistical significance were observed upon salt addition. [d] Value determined from NMR is K_a = 34 800 M^{-1}. [e] Value determined from NMR is K_a > 230 000 M^{-1} (axial phenyl linker resonances at 5.33 and 6.18 ppm were used for analyses).

monitoring (Fig. S15†). In the ^{1}H NMR spectra of **6c**, protons on the axial phenylene linker at 5.33 and 6.18 ppm shifted downfield upon the addition of K^+ up to 5.46 and 6.62 at a 1 : 1 ratio of **6c** : KOTf with $\Delta\delta$ = 0.13 and 0.44 ppm, respectively (Fig. 3). Further addition of K^+ did not alter the position of the resonances. The shift can be explained by the fact that coordination of the cation leads to a lower ability of nitrogen to donate electrons to phenylene, which leads to a magnetic deshielding effect. Similarly, the signal at approximately 3.27 ppm corresponding to the protons of $-CH_2-$ next to the nitrogen in the aza-crown shifted upfield to 2.97 ppm ($\Delta\delta$ = −0.30 ppm) at a 1 : 1 ratio of **6c** : KOTf and did not move further at higher salt concentrations. This opposite shift of **6c** resonances was probably caused by the reduction of aza-crown conformational flexibility in conjunction with changes in the electron density on the nitrogen atom upon cation encapsulation. The interaction of **6c** with Ba^{2+} (Fig. S13†) showed a similar pattern with chemical shift differences of $\Delta\delta$ = 0.16 and 0.61 ppm for phenylene and $\Delta\delta$ = −0.19 ppm for aliphatic signals of aza-crown protons. Similar cation-induced NMR shifts were also observed in the literature for aza-crown containing benzyl sidearms.[35] No changes in the ^{1}H NMR of the always-ON control **6d** were noticed (Fig. S14†). NMR studies with **6c** and its negative control **6d**, thus, unequivocally proved 1 : 1 binding stoichiometry in the case of **6c**/K^+ and **6c**/Ba^{2+}. This is in agreement with the results from Job's plot (*i.e.*, method of continuous variations, Fig. S15†), where the 1 : 1 stoichiometry was further confirmed independently for **6b**/Na^+, **6b**/Ba^{2+}, **6c**/K^+ and **6c**/Ba^{2+} using the fluorescence emission intensity.

The binding strength between SubPcs **6a–c** and individual cations was then analyzed using a 1 : 1 host–guest binding model,[36,37] with the apparent binding constant K_a. The constant is apparent due to the presence of MeOH in the cation stock solution, which also interacts with SubPc's aza-crown[38] unit (more details are given below). The binding isotherms are plotted in Fig. 2c, d and Fig. S16† and the actual values are given in Table 1 and Table S1.†

Size-driven recognition of cations took place only for alkali metal cations, whereas limited size preference was observed in the group of alkaline earth metal cations. For example, **6c** bearing a 1-aza-6-crown-18 moiety is switched ON by K^+ and not by smaller cations, such as Na^+ and Li^+ (where the binding constants are small). Although the FEF increases in the presence of both K^+ and Li^+, in the case of Li^+ this occurs only at high concentrations since K_a = 5.7 M^{-1}.

SubPc **6b** with a 1-aza-5-crown-15 moiety prefers, on the other hand, Na^+ over K^+, which is documented by higher FEF and K_a values for **6b**/Na^+ interaction than those for **6b**/K^+. The smallest analogue **6a** with a 1-aza-4-crown-12 moiety recog-

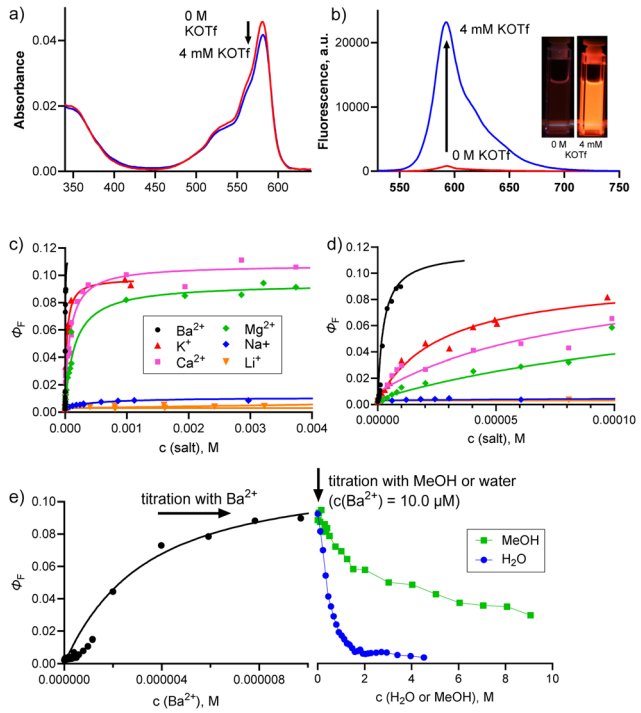

Fig. 2 Changes in the (a) absorption and (b) fluorescence emission spectra of **6c** (1 μM) upon titration with KOTf. (c) Increase in Φ_F of **6c** (1 μM) upon the addition of an analyte (in the form of triflates). (d) Enlarged part of the graph up to 0.1 μM of triflate salt. (e) Increase in Φ_F of **6c** (1 μM) upon the addition of Ba^{2+} triflate (titration done to reach the plateau phase where $c(Ba^{2+})$ = 10 μM), followed by titration by water or methanol ($c(Ba^{2+})$ = 10 μM). The excitation wavelength of 505 nm was used for all experiments shown in this figure.

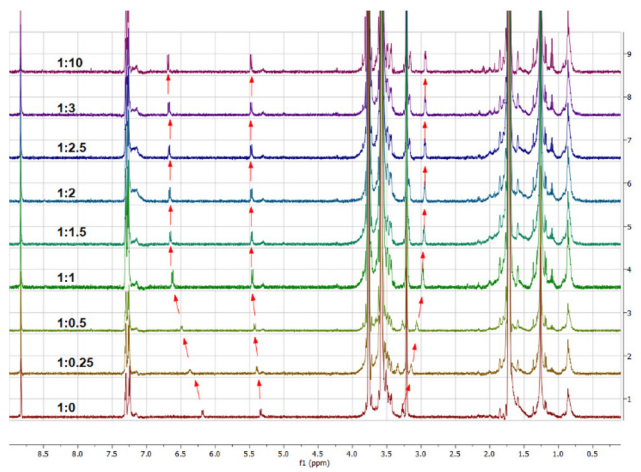

Fig. 3 ^{1}H NMR spectra (600 MHz, THF-d_8/MeOH-d_4 5 : 2) of **6c** with KOTf at different SubPc : salt ratios.

nized Li^+ over the others; however, K_a was 9.9 M^{-1} only, indicating that this sensor is selective for Li^+ but can be switched ON only at high Li^+ concentrations.

Alkaline earth metal cations were coordinated to **6a–c** more tightly than alkali metal cations, which was obvious from both high FEF values reaching the value of the control compound **6d** and the high K_a values (approximately in thousands of M^{-1}) (see Table 1 and Table S1†). A similar trend has been published before using different methods (*i.e.*, absorption[39] and fluorescence[8] spectroscopy, polarography[40] or laser infrared multiple photon dissociation spectroscopy[41]). This can be explained by the fact that alkaline earth metal cations are roughly similar in size to alkali metals, but being divalent cations, they possess a larger positive charge. As a result, their interaction with the aza-crown moiety is stronger, resulting in higher FEF and K_a values. Surprisingly, the binding of Ba^{2+} was, in our case, abnormally strong since the K_a values were determined to be 192 000, 13 900 and 384 000 M^{-1} for **6a**, **6b** and **6c**, respectively. This gives us a great starting point for follow-up studies on Ba^{2+} sensors.

Importantly, there was a decrease in the fluorescence emission upon the addition of water or MeOH into the solution of the already switched-ON SubPc **6c** (1 μM) by Ba^{2+} (10.0 μM), as seen in Fig. 2e. This effect was moderate for MeOH and more substantial for water. This indicates that more polar molecules bind more strongly to the aza-crown unit[38] and knock out the Ba^{2+} cation, which enables fluorescence quenching *via* PET. This is further depicted by the weakened fluorescence response (and lower sensitivity) of a **6c** solution containing a defined amount of water when titrated with Ba^{2+} cations (Fig. S17a†). Similar behaviour can also be observed for K^+ (Fig. S17b†). These results suggest that the ambient environment plays a very important role in cation sensing, and it is essential to investigate the sensing capability of the sensors in aqueous media to assess their impact as fluorescence sensors.

Metal cation sensing in water

SubPcs are too hydrophobic sensor molecules to be used in water without losing their monomeric character and fluorescence properties. To overcome these limitations, compound **6c**, chosen as a model compound of the series, and **6d**, a control compound always in the ON state, were integrated into ~10 nm-sized Tween 80 micelles. Tween 80 is a common non-ionic surfactant and emulsifier, and the characteristics of prepared micelles in water are presented in Table S2 and Fig. S18 and S19.† The absorption spectra of **6c** and **6d** in micelles corresponded well with their absorption spectra in THF (Fig. 4a), which proves the monomeric character of both compounds under aqueous conditions. Surprisingly, the fluorescence intensity of **6c**/**Tween 80** was not efficiently quenched (Φ_F = 0.04), indicating a specific interaction of the 1-aza-6-crown-18 moiety with the solvent. As a result of the high initial Φ_F value, the addition of KCl led only to a small increase in the fluorescence intensity (data not shown). Explanation consists of the fact that aza-crown nitrogen has the character of weakly basic aromatic amine and can be partially protonated in used deionized water of approximately pH 6. We assumed that nitrogen protonation leads to the reduction of the efficacy of PET even in the OFF state and, therefore, to a high initial Φ_F value. To prove that, we investigated the fluorescence intensities of the **6c**/**Tween 80** and **6d**/**Tween80** at different pH values, and

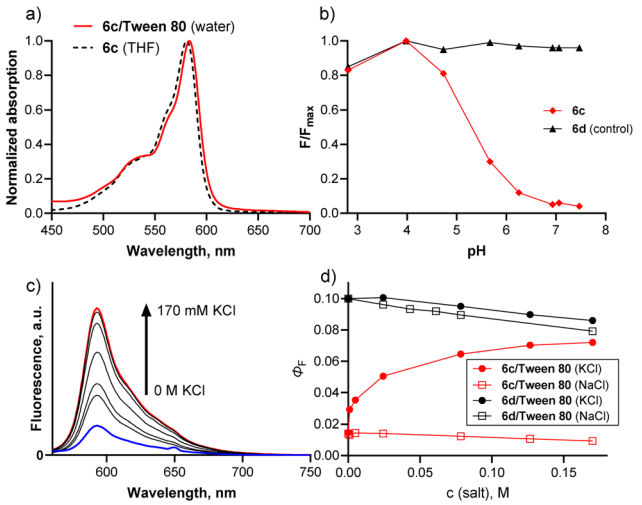

Fig. 4 (a) Normalized absorption spectra of **6c** in THF and **6c/Tween 80** in deionized water (pH~6). (b) Changes in the fluorescence intensity in aqueous media of different pH values. (c) Changes in the fluorescence emission spectra of **6c/Tween 80** upon the addition of KCl (Tris buffer, pH ~8). (d) Changes in fluorescence quantum yields during titration with KCl or NaCl (d). The excitation wavelength of 530 nm was used for all experiments.

indeed, the a considerable decrease of fluorescence intensities, *i.e.*, high efficacy of PET, of **6c/Tween80** was restored at pH values above 7 (Fig. 4b). Since the physiological pH is 7.4, the effect of protonation should not affect the sensor's properties in the biological environment.

Based on the above results, the sensing ability of **6c/Tween 80** was investigated in TRIS buffer at approximately pH 8 to eliminate protonation of aza-crown nitrogens. In agreement with the fluorescence behaviour of **6c** in THF, the fluorescence emission of **6c/Tween 80** in Tris buffer was weak (the OFF state, Φ_F = 0.014), and responded to the addition of KCl (up to Φ_F = 0.072) (Fig. 4c and d), but not to the addition of NaCl (Φ_F = 0.017) (Fig. S20†). In contrast, the always-ON control **6d/Tween 80** exhibited constant fluorescence emission (Φ_F = 0.10) irrespective of the pH value (Fig. 4b), and slight fluorescence quenching with increased concentrations of NaCl (Φ_F = 0.089) or KCl (Φ_F = 0.095) (Fig. 4d, Fig. S20†). The results of **6c/Tween 80**, showing approximately a 5-time increase of Φ_F in the presence of KCl, proved that prepared derivatives can be transferred to aqueous media using micelles as delivery systems without losing their sensing abilities.

Conclusions

A straightforward synthetic method for introducing aza-crown moieties at the axial position of SubPcs or SubAzaPcs was developed. Since the synthesized SubAzaPcs had blue-shifted absorption and emission spectra, were less stable during purification processes, and were less photostable when compared with the corresponding SubPc derivatives, the sensing ability towards alkali and alkaline earth metal cations was studied in detail only in a series of SubPc aza-crown derivatives **6a–6c**. SubPc sensors were switched ON in the presence of sensitive analytes, that was monitored as an increase in Φ_F. Size preference was observed only in the case of alkali metal cations, while alkaline earth metal cations were bonded regardless of their size. High molar absorption coefficients of the studied SubPc derivatives ($\log \varepsilon$ ~4.7 dm^3 mol^{-1} cm^{-1}), high fluorescence enhancement factors of selective anions (FEF up to 107), and high fluorescence quantum yields in the ON state (Φ_F up to 0.15) rank these derivatives among promising fluorescence sensors. Interestingly, the binding of Ba^{2+} was extraordinarily strong, making some of these derivatives promising targets for follow-up studies aimed to monitor Ba^{2+} in the environment.

Importantly, we have shown that assessment of the selectivity of a sensor towards an analyte requires collecting characteristics such as the FEF, Φ_F in the ON state, and the corresponding K_a values and evaluating them together. It can be documented by the behavior of **6c**. This derivative showed a strong fluorescence emission increase upon meeting Li^+, K^+, Ca^{2+}, Mg^{2+} and Ba^{2+}; however, only K^+ and Ba^{2+} ions exhibited reasonable K_a values. Since the levels of Ba^{2+} in plasma are negligible,[42] **6c** can be considered as a promising fluorescence sensor candidate for the selective recognition of K^+ levels in human fluids.

This work also highlighted the need to study the sensing ability of sensors in aqueous environments, since the presence of water (and other polar molecules such as MeOH) significantly altered the binding of cations to aza-crowns. Finally, the present study opened new directions for broader applications of SubPcs in fluorescence sensing, since these derivatives provide photostable fluorophores with advantageous spectral properties, and the sensing ability can be transposed into aqueous media. Their great advantage is that recognition moieties can be attached at the axial position, whereas their peripheral sites on signalling moieties may be used to tune the spectral and physico-chemical properties.

Experimental

General

All chemical reagents were purchased from certified suppliers (Sigma-Aldrich, TCI, Acros Organic, Fluorochem) and used as received. All the organic solvents used in the synthesis were of analytical grade. Thin-layer chromatography was performed on Merck aluminum sheets coated with silica gel 60 F254. Merck Kieselgel 60 (0.040–0.063 mm) was used for column chromatography. The infrared spectra were measured on a Nicolet 6700 spectrometer in the ATR mode. The ^{1}H and ^{13}C NMR spectra were recorded on a VNMR S500 NMR spectrometer or a Jeol JNM-ECZ600R. The chemical shifts are reported as δ values in ppm and are indirectly referenced to $Si(CH_3)_4$ *via* the signal from the solvent. *J* values are given in Hz. The UV–vis spectra were recorded using a Shimadzu UV-2600 spectrophotometer (Shimadzu, Kyoto, Japan). Fluorescence spectra were recorded

using an FS5 spectrofluorometer (Edinburgh Instruments, Edinburgh, UK). A UHPLC Acquity UPLC I-class system (Waters, Millford, USA) coupled to a high-resolution mass spectrometer (HRMS) Synapt G2Si (Waters, Manchester, UK) based on Q-TOF were used for HRMS spectra measurement. Chromatography was carried out using an Acquity UPLC BEH C18 column (2.1 × 50 mm, 1.7 μm) or an Acquity UPLC BEH C4 (2.1 × 50 mm, 1.7 μm, 300 Å) columns for molecules up to or above 1200 *m*/*z*, respectively, using gradient elution with acetonitrile and 0.1% formic acid at a flow rate of 0.4 ml min^{-1}. Electrospray ionization was operated in positive mode. The ESI spectra were recorded using leucine-enkephalin as a lock mass reference and sodium formate (in the range 50–1200 *m*/*z*) or sodium iodide (in the range 50–2000 *m*/*z*) for mass calibration.

The compounds **1**,[43] **4**,[27,28] **5**,[29] **6d**[25] and **7d**[25] were synthesized according to the previously reported procedures.

Synthesis

General procedure for 2a–c. The conditions were adopted from the literature.[44] A mixture of 2-(4-bromophenoxy)tetrahydro-2*H*-pyran (**1**) (256 mg, 1 mmol), $Pd_2(dba)_2$ (9.2 mg, 0.01 mmol), NaO*t*Bu (135 mg, 1.4 mmol), and DavePhos (11.8 mg, 0.03 mmol) under an argon atmosphere was preheated to approximately 60 °C. A solution of the aza-crown ether (1.14 mmol) in 2 mL of anhydrous toluene was added to the mixture and stirred at 80 °C for 12 h. The reaction mixture was then cooled to room temperature, diluted with dichloromethane (60 mL) and filtered through Celite. The crude product was purified using column chromatography on silica using ethyl acetate as an eluent.

10-(4-((Tetrahydro-2*H*-pyran-2-yl)oxy)phenyl)-1,4,7-trioxa-10-azacyclododecane (2a). Reaction time, 8 hours; yield 285 mg, (81%) as pale yellow-coloured oil. ^{1}H NMR (600 MHz, methanol-d_4) δ 6.89 (d, J = 9.6 Hz, 2H), 6.70 (d, J = 9.6 Hz, 2H), 5.20 (t, J = 3.6 Hz, 1H), 3.97–3.91 (m, 1H), 3.77 (t, J = 4.9 Hz, 4H), 3.67–3.62 (m, 4H), 3.62–3.58 (m, 4H), 3.59–3.53 (m, 1H), 3.46 (t, J = 4.9 Hz, 4H), 2.01–1.92 (m, 1H), 1.87–1.79 (m, 1H), 1.79–1.73 (m, 1H), 1.69–1.61 (m, 2H), 1.63–1.54 (m, 1H). ^{13}C NMR (151 MHz, methanol-d_4) δ 149.97, 145.81, 119.05, 115.10, 99.20, 72.33, 71.03, 70.89, 63.30, 53.99, 31.75, 26.43, 20.24. IR (ATR): ν_{max} (cm^{-1}) 2949, 2857, 2360, 1227, 1123, 1111, 1022, 921, 823. HRMS (ESI) calculated for $C_{19}H_{29}NO_5 + H^+$ 352.2119, found 352.2116 $[M + H]^+$.

13-(4-((Tetrahydro-2*H*-pyran-2-yl)oxy)phenyl)-1,4,7,10-tetraoxa-13-azacyclopentadecane (2b). Reaction time, 12 hours; yield, 364 mg (92%) as pale yellow-coloured oil. ^{1}H NMR (600 MHz, methanol-d_4) δ 6.90 (d, J = 9.4 Hz, 2H), 6.62 (d, J = 9.0 Hz, 2H), 5.19 (t, J = 3.6 Hz, 1H), 3.97–3.90 (m, 1H), 3.70 (t, J = 6.1 Hz, 4H), 3.65–3.60 (m, 12H), 3.58–3.54 (m, 1H), 3.50 (t, J = 6.1 Hz, 4H), 2.01–1.93 (m, 1H), 1.86–1.80 (m, 1H), 1.79–1.73 (m, 1H), 1.68–1.61 (m, 2H), 1.60–1.54 (m, 1H). ^{13}C NMR (151 MHz, methanol-d_4) δ 149.68, 144.84, 119.32, 113.95, 99.27, 72.05, 71.21, 71.02, 70.13, 63.28, 53.70, 31.76, 26.45, 20.25. IR (ATR): ν_{max} (cm^{-1}) 2939, 2867, 1512, 1355, 1235, 1125, 1036, 971, 921. HRMS (ESI) calculated for $C_{21}H_{33}NO_6 + H^+$ 396.2381, found 396.2377 $[M + H]^+$, 418.2195 $[M + Na]^+$.

16-(4-((Tetrahydro-2*H*-pyran-2-yl)oxy)phenyl)-1,4,7,10,13-pentaoxa-16-azacyclooctadecane (2c). Reaction time, 12 hours; yield, 339 mg (77%) as pale yellow-coloured oil. ^{1}H NMR (600 MHz, methanol-d_4) δ 6.90 (d, J = 9.2 Hz, 2H), 6.68 (d, J = 9.0 Hz, 2H), 5.21 (t, J = 3.6 Hz, 1H), 3.98–3.91 (m, 1H), 3.69–3.60 (m, 20H), 3.62–3.54 (m, 1H), 3.52 (t, J = 6.0 Hz, 4H), 2.02–1.92 (m, 1H), 1.88–1.80 (m, 1H), 1.80–1.73 (m, 1H), 1.67–1.62 (m, 2H), 1.61–1.54 (m, 1H). ^{13}C NMR (151 MHz, methanol-d_4) δ 149.99, 145.08, 119.23, 114.91, 99.22, 71.76, 71.74, 71.70, 71.64, 70.11, 63.31, 52.99, 31.74, 26.43, 20.24. IR (ATR): ν_{max} (cm^{-1}) 2940, 2869, 2557, 1512, 1234, 1109, 1036, 971, 921, 816. HRMS (ESI) calculated for $C_{23}H_{37}NO_7 + H^+$ 440.2643, found 440.2647 $[M + H]^+$, 462.2462 $[M + Na]^+$.

General procedure for 3a–c. Compound **2a–c** (0.075 mmol), and *p*-toluenesulfonic acid (0.075 mmol) in methanol (1.2 mL) were stirred under an argon atmosphere for 2 hours at room temperature. On completion, the product was extracted with chloroform (30 mL) and a saturated aqueous solution of $NaHCO_3$ (30 mL). The organic layer was collected, and the crude product was purified using column chromatography on silica. The yields and mobile phases are mentioned at each compound below.

4-(1,4,7-Trioxa-10-azacyclododecan-10-yl)phenol (3a). Mobile phase: triethyl acetate/ethyl acetate 1 : 45; yield 15 mg (74%) as a light pink oil. ^{1}H NMR (500 MHz, DMSO-d_6) δ 8.48 (s, 1H), 6.61–6.57 (m, 2H), 6.57–6.54 (m, 2H), 3.67 (t, J = 5.0 Hz, 4H), 3.56–3.50 (m, 8H), 3.36 (t, J = 5.0 Hz, 4H). ^{13}C NMR (126 MHz, DMSO-d_6) δ 148.26, 141.92, 115.69, 113.77, 70.83, 69.30, 69.04, 52.07. IR (ATR): ν_{max} (cm^{-1}) 2924, 2856, 1514, 1360, 1226, 1125, 1089, 1067, 817, 677, 646. HRMS (ESI) calculated for $C_{14}H_{21}NO_4 + H^+$ 268.1544, found 268.1547 $[M + H]^+$, 290.1363 $[M + Na]^+$.

4-(1,4,7,10-Tetraoxa-13-azacyclopentadecan-13-yl)phenol (3b). Mobile phase: chloroform/ethyl acetate 3 : 2; yield 21 mg (87%) as a light pink oil. ^{1}H NMR (500 MHz, DMSO-d_6) δ 8.45 (s, 1H), 6.64–6.57 (m, 2H), 6.51–6.44 (m, 2H), 3.58 (t, J = 6.1 Hz, 4H), 3.55–3.47 (m, 12H), 3.37 (t, J = 6.1 Hz, 4H). ^{13}C NMR (126 MHz, DMSO-d_6) δ 148.01, 140.99, 115.87, 112.78, 70.35, 69.44, 69.19, 68.36, 52.21. IR (ATR): ν_{max} (cm^{-1}) 2865, 1734, 1514, 1355, 1222, 1121, 938, 814, 734. HRMS (ESI) calculated for $C_{16}H_{25}NO_5 + H^+$ 312.1806, found 312.1810 $[M + H]^+$, 334.1629 $[M + Na]^+$.

4-(1,4,7,10,13-Pentaoxa-16-azacyclooctadecane-16-yl)phenol (3c). Mobile phase: ethyl acetate/methanol 95 : 15; yield 24 mg (89%) as a light pink oil. ^{1}H NMR (600 MHz, DMSO-d_6) δ 8.50 (s, 1H), 6.64–6.58 (m, 2H), 6.57–6.51 (m, 2H), 3.55–3.52 (m, 20H), 3.38 (t, J = 6.1 Hz, 4H). ^{13}C NMR (151 MHz, DMSO-d_6) δ 148.36, 141.27, 115.82, 113.67, 70.07, 70.06, 69.98, 69.92, 68.39, 51.40. IR (ATR): ν_{max} (cm^{-1}) 2866, 1514, 1351, 1249, 1112, 945, 816. HRMS (ESI) calculated for $C_{18}H_{29}NO_6 + H^+$ 356.2068, found 356.2065 $[M + H]^+$, 378.1887 $[M + Na]^+$.

General procedure for the synthesis of target macrocycles. The procedure was adopted from the literature[25] using a one-pot reaction procedure. Briefly, an equimolar amount of a 1 M

solution of BCl_3 in *p*-xylene was added to **4** (or **5**) upon stirring under an argon atmosphere. The reaction mixture was refluxed for 2 hours. Afterward, the solvent was removed under reduced pressure. The residue was then mixed with **3a–c** (3 equivalents) dissolved in anhydrous toluene, and the resulting mixture was refluxed under an argon atmosphere overnight. The crude product was purified using column chromatography on silica. The amounts of reactants, as well as mobile phases, are listed for each compound below.

SubPcs 6a. Compounds **4** (56 mg, 0.2 mmol) and **3a** (160 mg, 0.6 mmol), reaction time 10 h, mobile phase: dichloromethane/acetone 90 : 4, yield 18 mg (23%) of violet solid. ^{1}H NMR (600 MHz, $CDCl_3$) δ 8.89 (s, 6H), 7.32–7.29 (m, 12H), 7.27–7.25 (m, 18H), 6.21–6.18 (m, 2H), 5.42–5.39 (m, 2H), 3.68–3.66 (m, 4H), 3.60 (dd, J = 4.3, 2.3 Hz, 4H), 3.55 (td, J = 3.9, 2.4 Hz, 4H), 3.32 (t, J = 4.9 Hz, 4H). ^{13}C NMR (151 MHz, $CDCl_3$) δ 151.64, 143.04, 141.25, 130.23, 130.11, 128.15, 127.14, 124.21, 119.79, 113.50, 71.60, 70.03, 69.94, 52.99. IR (ATR): ν_{max} (cm^{-1}) 3648, 3545, 3524, 3502, 2926, 2854, 1731, 1511, 1455, 1439, 1163, 1068, 762, 724, 656. HRMS (ESI) calculated for $C_{78}H_{64}BN_7O_6 + H^+$, 1118.4560 found 1118.4568 $[M + H]^+$ 1118.4388 $[M + Na]^+$. λ_{max} (THF, log ε) 581 (4.762), 525 (sh), and 323 nm (4.441 dm^3 mol^{-1} cm^{-1}).

SubPc 6b. Compound **4** (56 mg, 0.2 mmol) and **3b** (190 mg, 0.6 mmol), reaction time 12 h, mobile phase: dichloromethane/acetone 9 : 1, yield 17 mg (22%) of violet solid. ^{1}H NMR (600 MHz, THF-d_8) δ 8.85 (s, 6H), 7.30–7.28 (m, 12H), 7.23–7.19 (m, 18H), 6.11–6.09 (m, 2H), 5.37–5.34 (2H, m), 3.51–3.49 (m, 8H), 3.47–3.44 (m, 8H), 3.27 (t, J = 6.1 Hz, 4H). ^{13}C NMR (151 MHz, THF-d_8) δ 152.926, 143.94, 142.474, 131.281, 131.142, 128.987, 127.948, 124.846, 120.676, 112.924, 72.377, 71.266, 71.118, 70.007, 53.599. IR (ATR): ν_{max} (cm^{-1}) 2927, 2854, 1732, 1454, 1439, 1242, 1163, 1123, 1069, 763, 701, 670. HRMS (ESI) calculated for $C_{78}H_{64}BN_7O_6 + H^+$, 1162.4822 found 1162.4833 $[M + H]^+$ 1184.4651 $[M + Na]^+$. λ_{max} (THF, log ε) 581 (4.732), 525 (sh), and 328 nm (4.334 dm^3 mol^{-1} cm^{-1}).

SubPc 6c. Compounds **4** (56 mg, 0.2 mmol) and **3c** (213 mg, 0.6 mmol), reaction time 12 h, mobile phase: dichloromethane/acetone 3 : 2, yield 21 mg (26%) of violet solid. ^{1}H NMR (600 MHz, THF-d_8) δ 8.84 (s, 6H), 7.33–7.30 (m, 12H), 7.26–7.22 (m, 18H), 6.17–6.14 (m, 2H), 5.37–5.33 (m, 2H), 3.53–3.50 (m, 12H), 3.48–3.45 (m, 8H), 3.31 (t, J = 6.1 Hz, 4H). ^{13}C NMR (151 MHz, THF-d_8) δ 152.93, 143.96, 142.48, 131.28, 131.16, 129.02, 127.98, 124.83, 120.65, 113.62, 71.96, 71.91, 71.89, 71.70, 70.15, 52.82. IR (ATR): ν_{max} (cm^{-1}) 3409, 2925, 2853, 1732, 1576, 1454, 1438, 1163, 1068, 1015, 762, 701, 612. HRMS (ESI) calculated for $C_{78}H_{64}BN_7O_6 + H^+$, 1206.5084 found 1206.5094 $[M + H]^+$ 1228.4918 $[M + Na]^+$. λ_{max} (THF, log ε) 582 (4.665), 525 (sh), and 328 nm (4.332 dm^3 mol^{-1} cm^{-1}).

SubAzaPc 7b. Compounds **5** (56.4 mg, 0.2 mmol) and **3b** (190 mg, 0.6 mmol) reaction time 8 h, mobile phase: dichloromethane/acetone 9 : 1, yield 9 mg (11%) of violet solid. ^{1}H NMR (600 MHz, THF-d_8) δ 7.79–7.75 (m, 12H), 7.43–7.37 (m, 18H), 6.14–6.10 (m, 2H), 5.38–5.33 (2H, m), 3.51–3.47 (m, 12H), 3.46–3.44 (m, 4H), 3.28 (t, J = 6.2 Hz, 4H). ^{13}C NMR (151 MHz, THF-d_8) δ 155.78, 149.92, 141.86, 140.22, 131.54, 130.21, 129.22, 122.57, 120.55, 113.06, 72.39, 71.29, 71.13, 69.96, 53.59. HRMS (ESI) calculated for $C_{78}H_{64}BN_7O_6 + H^+$, 1168.4537 found 1168.4543 $[M + H]^+$ 1190.4364 $[M + Na]^+$. λ_{max} (THF, log ε) 549 (4.557), 500 (sh) and 377 nm (4.420 dm^3 mol^{-1} cm^{-1}).

Spectral and photophysical studies in the presence of analytes. A volume of 25 μL of a stock solution of a SubPc (100 μM, THF) was transferred to 2.475 mL of THF in the cuvette (*i.e.*, c = 1 μM). Both absorption and emission spectra were measured (λ_{exc} = 505 nm). Appropriate analytes were added stepwise in the form of a triflate (stock solution in MeOH), and absorption and emission spectra were measured after each addition. The obtained data were analysed by the determination of Φ_F *via* the reference method using rhodamine 6G as the reference (Φ_F = 0.94 in EtOH[34]).

Photobleaching studies. Samples (1 μM, in THF) were prepared in the dark by the addition of 25 μL of the stock solution (100 μM, THF) to 2.45 mL of THF in the cuvette. The solution was then irradiated for specific times (100 W Xe-ozone free lamp, Newport) while stirring, using a water filter to remove heat. The absorption spectrum was measured after each irradiation step. Decomposition was monitored as a decrease in absorption intensity at Q band maximum (550 nm and 582 nm, for **7b** and **7d**, and for **6b** and **6d**, respectively, and 665 and 489 nm for ZnPc and FAM, respectively) as a function of irradiation time.

Job's method of continuous variation

Stock solutions of a SubPc (10 μM) and salt (10 μM) in a mixture of THF/MeOH 8 : 2 were prepared. A series of fluorescence measurements with different SubPc/salt ratios (18 measurements ranging between 1 : 4 and 4 : 1 ratios) with a constant total volume of 2.5 mL and total concentration of components of 10 μM ([SubPc] + [salt] = 10 μM) was performed. The final stoichiometry was determined from the Job's plot constructed from the dependence of $F_x - F_0$ on [analyte]/([analyte] + [SubPc]), where F_x refers to the fluorescence emission intensity of the SubPc/salt mixture and F_0 to the mixture where THF/MeOH 8 : 2 (without dissolved salt) was used instead of a salt stock solution.

Preparation of micelles. 0.1 mg of SubPc **6c** (or **6d**) and 200 mg of Tween 80 in DMSO (200 μL) were added dropwise to deionized water (5 mL). The resulting solution was left stirring for 18 hours. The size and zeta potential distributions of the micellar solutions in deionized water (pH ∼6) were determined using dynamic light scattering (DLS) on a particle size analyzer Zetasizer Nano ZS (Malvern, UK). Data are shown in the ESI.†

The effect of pH value on the fluorescence properties of SubPc/Tween 80. Several aqueous solutions adjusted to pH values from 3 to 9 either by acetic acid or pyridine were prepared. A volume of 1 mL of those solutions was mixed with 0.1 mL of a micelle **6c**/**Tween 80** (or **6d**/**Tween 80**), stirred for 30 seconds, and the fluorescence emission spectrum was measured (excitation wavelength 530 nm). The pH value of each sample was determined directly in the cuvette using a pH

meter Sentron SI 400 equipped with a MicroFET pH probe (Sentron, Leek, The Netherlands). The results were analysed as F/F_{max} as a function of the pH value, where F refers to the fluorescence intensity at a given pH value and F_{max} to the highest fluorescence intensity within the measurement (*i.e.*, at pH = 3.98).

Titration of SubPc/Tween 80 with KCl and NaCl. 1 mL of the prepared SubPc/Tween 80 micelle was diluted with 4 mL of Tris buffer (pH = 8.5) to prepare a stock solution of the dye. For titration, 2 mL of the stock solution was taken in a cuvette, to which increments of 1 M aqueous KCl and NaCl solutions were added, and their absorption and emission spectra were measured until maximum fluorescence was observed. Both control and sensor compounds were subjected to this procedure.

Author contributions

MAA – conducted the research and investigation process, specifically performed the experiments; JL – performed the calculations (association constants, *etc*.) and wrote the manuscript, KL and KK – prepared and characterized the micelles, and edited the manuscript; PS and PZ – conduced a critical review of the research hypothesis and wrote the draft of the manuscript; VN – formulated the research goals, provided mentorship, and wrote the manuscript.

Conflicts of interest

There are no conflicts to declare.

Acknowledgements

The financial support from the Czech Science Foundation (21-14919J), Russian Foundation for Basic Research (20-53-26004) and Charles University (SVV 260 666, PRIMUS/20/SCI/013) is gratefully acknowledged.

References

1 A. Sigel, H. Sigel and R. K. O. Sigel, in *The Alkali Metal Ions: Their Role for Life*, Springer, Cham, 2016, vol. 16, p. 628, DOI: 10.1007/978-3-319-21756-7.
2 P. Pathak, R. R. Srivastava, G. Keceli and S. Mishra, in *Strontium Contamination in the Environment*, ed. P. Pathak and D. K. Gupta, Springer International Publishing, Cham, 2020, pp. 227–243, DOI: 10.1007/978-3-030-15314-4_12.
3 M. Rajasekar, V. Ranjitha and K. Rajasekar, *Results Chem.*, 2023, **5**, 100850.
4 A. P. de Silva, H. Q. N. Gunaratne, T. Gunnlaugsson, A. J. M. Huxley, C. P. McCoy, J. T. Rademacher and T. E. Rice, *Chem. Rev.*, 1997, **97**, 1515–1566.
5 H. Niu, J. Liu, H. M. O'Connor, T. Gunnlaugsson, T. D. James and H. Zhang, *Chem. Soc. Rev.*, 2023, **52**, 2322–2357.
6 J. Li, D. Yim, W.-D. Jang and J. Yoon, *Chem. Soc. Rev.*, 2017, **46**, 2437–2458.
7 X. X. Zhang, R. M. Izatt, J. S. Bradshaw and K. E. Krakowiak, *Coord. Chem. Rev.*, 1998, **174**, 179–189.
8 L. Lochman, J. Svec, J. Roh and V. Novakova, *Dyes Pigm.*, 2015, **121**, 178–187.
9 L. Lochman, M. Machacek, M. Miletin, S. Uhlirova, K. Lang, K. Kirakci, P. Zimcik and V. Novakova, *ACS Sens.*, 2019, **4**, 1552–1559.
10 L. Lochman, J. Svec, J. Roh, K. Kirakci, K. Lang, P. Zimcik and V. Novakova, *Chem. – Eur. J.*, 2016, **22**, 2417–2426.
11 L. D. Lavis and R. T. Raines, *ACS Chem. Biol.*, 2008, **3**, 142–155.
12 R. Jenkins, M. K. Burdette and S. H. Foulger, *RSC Adv.*, 2016, **6**, 65459–65474.
13 V. Novakova, M. P. Donzello, C. Ercolani, P. Zimcik and P. A. Stuzhin, *Coord. Chem. Rev.*, 2018, **361**, 1–73.
14 V. Novakova, *J. Porphyrins Phthalocyanines*, 2022, **26**, 765–782.
15 M. H. Shi, J. Z. Chen and Z. Shen, *J. Porphyrins Phthalocyanines*, 2016, **20**, 1082–1089.
16 H. Gotfredsen, M. D. Kilde, M. Santella, A. Kadziola and M. B. Nielsen, *Mol. Syst. Des. Eng.*, 2019, **4**, 199–205.
17 E. van de Winckel, M. Mascaraque, A. Zamarron, A. J. de la Fuente, T. Torres and A. de la Escosura, *Adv. Funct. Mater.*, 2018, **28**, 10.
18 H. Xu, X. J. Jiang, E. Y. M. Chan, W. P. Fong and D. K. P. Ng, *Org. Biomol. Chem.*, 2007, **5**, 3987–3992.
19 H. Xu and D. K. P. Ng, *Chem. – Asian J.*, 2009, **4**, 104–110.
20 F. Yurt, T. Arslan, Z. Biyiklioglu, A. Tuncel, D. Ozel and K. Ocakoglu, *J. Drug Delivery Sci. Technol.*, 2020, **56**, 101567.
21 J. Demuth, L. Gallego, M. Kozlikova, M. Machacek, R. Kucera, T. Torres, M. V. Martinez-Diaz and V. Novakova, *J. Med. Chem.*, 2021, **64**, 17436–17447.
22 J. Labella and T. Torres, *Trends Chem.*, 2023, **5**, 353–366.
23 G. Lavarda, J. Labella, M. V. Martínez-Díaz, M. S. Rodríguez-Morgade, A. Osuka and T. Torres, *Chem. Soc. Rev.*, 2022, **51**, 9482–9619.
24 N. Kobayashi, T. Ishizaki, K. Ishii and H. Konami, *J. Am. Chem. Soc.*, 1999, **121**, 9096–9110.
25 I. A. Skvortsov, P. Zimcik, P. A. Stuzhin and V. Novakova, *Dalton Trans.*, 2020, **49**, 11090–11098.
26 S. Xu, K. C. Chen and H. Tian, *J. Mater. Chem.*, 2005, **15**, 2676–2680.
27 T. V. Dubinina, S. A. Trashin, N. E. Borisova, I. A. Boginskaya, L. G. Tomilova and N. S. Zefirov, *Dyes Pigm.*, 2012, **93**, 1471–1480.
28 T. V. Dubinina, M. S. Belousov, S. S. Maklakov, V. I. Chernichkin, M. V. Sedova, V. A. Tafeenko, N. E. Borisova and L. G. Tomilova, *Dyes Pigm.*, 2019, **170**, 107655.
29 H. W. Rothkopf, D. Wohrle, R. Muller and G. Kossmehl, *Chem. Ber.*, 1975, **108**, 875–886.

30 V. Novakova, P. Reimerova, J. Svec, D. Suchan, M. Miletin, H. M. Rhoda, V. N. Nemykin and P. Zimcik, *Dalton Trans.*, 2015, **44**, 13220–13233.
31 H. Xu, W. K. Chan and D. K. P. Ng, *Synthesis*, 2009, 1791–1796.
32 V. V. Travkin, D. A. Semikov, P. A. Stuzhin, I. A. Skvortsov and G. L. Pakhomov, *Appl. Sci.*, 2023, **13**, 1211.
33 I. A. Skvortsov, U. P. Kovkova, Y. A. Zhabanov, I. A. Khodov, N. V. Somov, G. L. Pakhomov and P. A. Stuzhin, *Dyes Pigm.*, 2021, **185**, 108944.
34 R. F. Kubin and A. N. Fletcher, *J. Lumin.*, 1982, **27**, 455–462.
35 K. W. Chi, K. T. Shim, H. H. U. Lee and Y. J. Park, *Bull. Korean Chem. Soc.*, 2005, **26**, 393–398.
36 K. Hirose, *J. Inclusion Phenom. Macrocyclic Chem.*, 2001, **39**, 193–209.
37 T. H. Ngo, J. Labuta, G. N. Lim, W. A. Webre, F. D'Souza, P. A. Karr, J. E. M. Lewis, J. P. Hill, K. Ariga and S. M. Goldup, *Chem. Sci.*, 2017, **8**, 6679–6685.
38 H.-J. Buschmann, R.-C. Mutihac and E. Schollmeyer, *J. Solution Chem.*, 2010, **39**, 291–299.
39 S. H. Mashraqui, S. Sundaram, T. Khan, S. Ghadigaonkar and K. Poonia, *J. Inclusion Phenom. Macrocyclic Chem.*, 2008, **62**, 81–90.
40 M. Hojo, I. Hisatsune, H. Tsurui and S.-i. Minami, *Anal. Sci.*, 2000, **16**, 1277–1284.
41 F. Gámez, P. Hurtado, B. Martínez-Haya, G. Berden and J. Oomens, *Int. J. Mass Spectrom.*, 2011, **308**, 217–224.
42 M. Łukasik-Głębocka, K. Sommerfeld, A. Hanć, A. Grzegorowski, D. Barałkiewicz, M. Gaca and B. Zielińska-Psuja, *J. Anal. Toxicol.*, 2014, **38**, 380–382.
43 S. Xu, L. Mao, P. Ding, X. Zhuang, Y. Zhou, L. Yu, Y. Liu, T. Nie, T. Xu, Y. Xu, J. Liu, J. Smaill, X. Ren, D. Wu and K. Ding, *Bioorg. Med. Chem.*, 2015, **23**, 3751–3760.
44 X.-X. Zhang and S. L. Buchwald, *J. Org. Chem.*, 2000, **65**, 8027–8031.